

# A new approach to acoustic insulation materials characterisation based on X-ray tomographic images and LBM simulations

*P. Lamary\*<sup>†</sup>, R. N. Rodrigues\*, R. A. Bezerra\*, E. P. Deus\*, B. N. Huallpa\*\* and F. C. Bannwart\*\*\**

*\* Federal University of Ceara, Center of Technology, CE, Brasil*

*\*\* Federal University of Lavras, Engineering Department, MG, Brasil*

*\*\*\* University of Campinas, School of Engineering, SP, Brasil*

pierre.lamary@ufc.br

<sup>†</sup>Corresponding author

## Abstract

A sample of a fibrous material is considered and the objective is the determination of two main characteristics of the material: the porosity and the static airflow resistivity. First, from 2D X-Ray tomographic images of the sample, the porosity is deduced. Next, the same images are used as the lattice of the Lattice Boltzmann Method (LBM) to carry out fluid dynamic calculations. The foundation of the method and specific developments we did, are presented. The results obtained are compared with characterizations using a porosity-meter and a resistivity-meter and show that they are very consistent.

## 1. Introduction

Acoustic insulation materials such as foam, glass wool, felt, perforated sheets, are used in aeronautics to reduce noise in commercial and general aviation air-crafts for passengers and crews comfort. In the aerospace sector, they can be used in launchers space fairing to reduce the internal noise and preserve the integrity of the payload, at the time of launching the rocket. The study of these systems is, in particular, carried through numerical simulations where it is needed to know the intrinsic characteristic of each components, namely, air domains, structural parts and poro-elastic acoustic materials. For the latter, the question is problematic because there are no standard acoustic materials, each ones differs from the others, and sometimes the process of manufacturing the material does not allow to recreate a material to the identical. The question to explore characterisation methods is therefore of primary interest. The proposed approach is based on the acquisition of tomographic images of the material and on Lattice Boltzmann Method (LBM) fluid dynamics calculations. A sample of a fibrous material is considered and the objective is the determination of two main characteristics of the material: the porosity and the static airflow resistivity.

## 2. Porosity

Porosity is defined as the ratio of the volume occupied by the fluid phase (usually air) to the total porous material volume, which also embraces the solid frame phase.<sup>2</sup> Porosity must be measured or computed for a representative volume of the acoustic material. A representative volume has a characteristic length much smaller than the wavelength of the waves in the audio frequency range and much larger than the random microscopic features of the material, so that average properties of the homogenized material can be obtained. Traditional methods usually applied to experimentally estimate porosity can be classified in two types. Direct methods consist in the immersion of a porous material sample in a incompressible fluid (typically water) and computing the volume ratio between the fluid phase and the entire sample.<sup>1</sup> Otherwise, if the mass density of the solid phase is known and homogeneous, from the weight of the sample, the volume of the solid frame can be computed and subtracted from the total volume obtained from the sample external geometry. More precise methods are based upon gas expansion in cavities with known volume and pressure measurements, such as in the Boyle's Law Porosimeter.<sup>8</sup>

The specimen used in this work was cut from a board made of coconut fibres recovered with natural latex produced by a local manufacturer (Coquim, Sao Paulo, Brazil). Figure 1 shows a cylindrical cut done in the fibres board. The extracted cylindrical sample will be use for reference tests using a porosity-meter and a resistivity-meter.

SHORT PAPER TITLE



Figure 1: Coconut fibre material under study.

The hexaedric sample will be used in the tomographic device. As will be explained later, the X-ray Tomography was able in our case to detect the fluid and solid phase of our material. The Figure 2 shows a 3D image reconstruction of our sample provided by the tomography device software suite. The sample size ( $50 \times 50 \times 50 \text{ mm}^3$ ) was selected in order to preserve the characteristics of the original arrangement of the compacted fibres and to allow measurement in acoustic devices. The softwares associated with X-ray tomography are also capable of reconstructing the samples in the form of finite elements, surface elements of the fibres surface, volume elements for the volume of the fibres and of the fluid domains. Fig. 3 and Fig. 4 show the mesh obtained when importing the 3D mesh data of the fibres in our own FE software. Fig. 3 shows the full sample, Fig. 4 is a zoom showing the tetrahedrons. Using 3D meshes is not the approach followed in this paper but this feature could be interesting for one who would like to connect X-ray tomography to finite element or to finite volume computations.

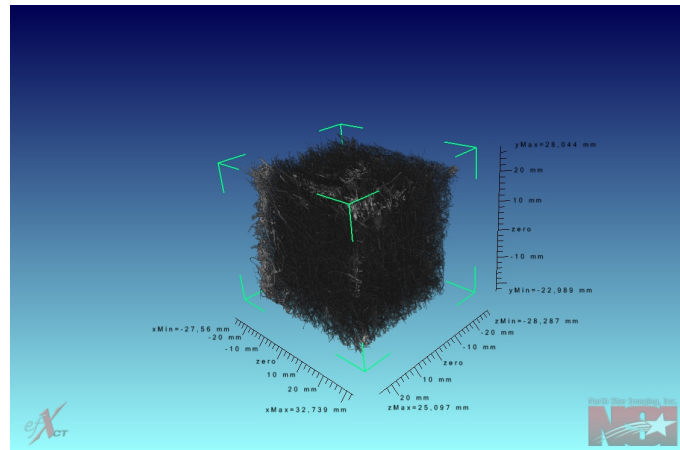


Figure 2: Porous sample under study - Tomographic 3D image reconstruction.

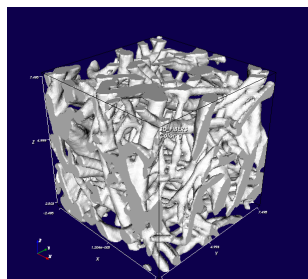


Figure 3: 3D mesh reconstruction - Full sample.

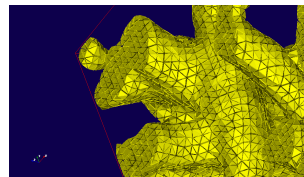


Figure 4: Tetrahedral elements - Zoom.

Our approach is based on basic data provided by X-ray tomography, that is to say, captures of gray-scaled slice images. The control of fibres separation of the fluid phase is performed by our own image post-processing analysis. The directly obtained X-ray CT images reveal 2D transversal slices of a sample,<sup>6</sup> sequentially numbered. Each image

is formed according to the X-ray attenuation dependency on the local material density through which the radiation is transmitted. For high energy X-rays (above 100 kV),<sup>9</sup> those images are associated to the so-called CT number and correlated to mass density. Therefore, in principle it is possible to estimate the porosity of a sample of porous material using CT images. If an acoustic material is composed of solid and fluid (air) phases, the solid phase is likely to have the higher density, which makes it distinguishable by contrast. Porosity is generally defined as the percentage of the air volume to the total volume, but could be defined, in an equivalent manner, as the proportion of the surface area of the fluid to the total area. That is what is done in this study. As a 2D slice image is less representative (in our case and generally) than the total chosen volume, the final porosity is computed as the mean of the porosity of several slice images. From the acquisition process, the sample is cropped to (40x40x40mm<sup>3</sup>). Figure 5 shows a slice image obtained using X-ray CT tomography. The dimension of a slice of this 3D image is therefore 40x40mm<sup>2</sup> with a pixel size of 46.1x46.1μm<sup>2</sup>. The thickness is 46.1μm. The clear spots correspond to the denser material (fiber), while the dark gray are the pores (fluid). Then, the 2D images were submitted to the process thresholding (transformation of the gray scale image to binary scale) using different methods that software imageJ offers. Figure 6 shows the result obtained when using the Otsu's thresholding method. From this, the porosity can be evaluated. Results will be given for a set of images.

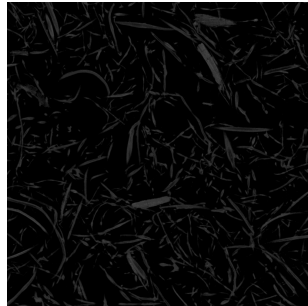


Figure 5: Slice number 500  
- Original image.



Figure 6: Slice number 500  
- Processed image.

### 3. Resistivity

When fluid goes slowly through pores, resistive phenomena induced by viscous friction are predominant and those forces balance with the fluid velocity. The pertinent parameter to describe this phenomena is the permeability of the medium, which is expressed by the Darcy's law. Written in an up-to-date form, the permeability  $\mathbf{k}$  is a second order tensor that we may write in Cartesian coordinates as

$$k_{ij} = -\frac{\eta}{p_{,j}} \langle v_i \rangle, \quad (1)$$

where  $v_i$  is the outflow speed field in the  $i$  direction,  $\langle \cdot \rangle$  is the volume average,  $\langle v_i \rangle = \phi \frac{\int_A v_i da}{\int_A da}$ , with  $\phi$  being the porosity and  $A$  being the area in 2D (or the volume in 3D) of the fluid part, and  $p_{,j}$  is the gradient pressure in the  $j$  direction. This gradient applies as a field all over the wet fluid domain. From this, the static airflow resistivity  $\sigma$ , which is also a second order tensor, can be related to  $\mathbf{k}$  as

$$\sigma_{ij} = \eta (k_{ij})^{-1}. \quad (2)$$

An acoustic material is generally manufactured in layer form, and the fabrication process may turn the layer orthotropic. If its principal directions are priorly known, tests or computation shall be carried out in those directions to directly express Eqs. 2 and 3, for instance. The permeability and resistivity tensors also possess the propriety of symmetry. The reader can refer to,<sup>4</sup> where experimental and numerical procedures are presented to characterize anisotropic materials. Neglecting the non-diagonal terms of  $\mathbf{k}$ , Eq. 2 can be solved as

$$\sigma_{ii} = \frac{\eta}{k_{ii}}, \quad (3)$$

with  $i \in \{1, 2\}$  for our 2D simulations. The mean value of the tensor defined as  $\sigma = (\sigma_{11} + \sigma_{22})/2$  is considered as our final indicator. To recover the 3D situation, several slices of a sample are considered, each slice being a 2D image

## SHORT PAPER TITLE

treated by a 2D calculation. Statistic mean values are given to approximate the global resistivity of the 3D sample. The Lattice Boltzmann Method (LBM) can be seen as a spacial and temporal finite difference method which takes benefit of a mesh (the lattice) that has to be strictly constructed with square elements with  $\Delta x = \Delta y = \Delta t$  for each element. Doing this, it is possible to solve the Boltzmann transport equation

$$\frac{\partial f}{\partial t} + \vec{v} \cdot \vec{\nabla} f = \Omega. \quad (4)$$

This equation is an equilibrium equation where  $f(\vec{x}, t)$  is the particle distribution function,  $\vec{v}(\vec{x}, t)$  is the particle velocity, and  $\Omega$  is the collision operator. The equilibrium is found iteratively. The main references used in this section are.<sup>3,5,10</sup> Using the D2Q9 model, shown in Fig. 7, the particle is restricted to stream in 9 possible directions described by the microscopic velocities  $\vec{e}_i$ , where the index  $i \in \{0, 1, 2, \dots, 8\}$ , with  $i = 0$  being attributed to the particle at rest. For each direction is also associated a probability function  $f_i$ . As important remarks: the vectors  $\vec{e}_i$  do not change during the process, in opposition to their associated distribution functions; the vectors  $\vec{e}_i$  on the diagonals are of  $\sqrt{2}$  length, while the others are unitary. The macroscopic fluid density  $\rho(\vec{x}, t)$  and the macroscopic velocity  $\vec{v}(\vec{x}, t)$  at each Lattice node

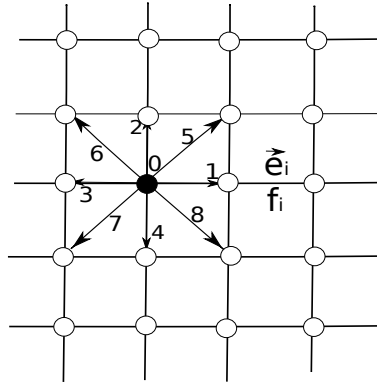


Figure 7: D2Q9 discretization scheme.

can be extracted from the probability distribution functions of the particle by the equations

$$\rho = \sum_i f_i, \quad \rho \vec{v} = \sum_i f_i \vec{e}_i, \quad (5)$$

and the pressure  $p$  can be evaluated from the density as  $p = \rho c_s^2$ , where  $c_s = 1/\sqrt{3}$  is the lattice speed of sound. Using the D2Q9 discretization and the Bhatnagar-Gross-Krook (BGK) collision model (that suffices for laminar single phase flows), Eq. 4 can be rewritten as

$$f_i(\vec{x} + c\vec{e}_i\Delta t, t + \Delta t) - f_i(\vec{x}, t) = -\frac{f_i(\vec{x}, t) - f_i^{eq}(\vec{x}, t)}{\tau}, \quad (6)$$

with  $\tau$  being a relaxation time, and  $f_i^{eq}$  the equilibrium distribution. Reorganizing Eq. 6 allows for the calculation of the distribution at  $t + \Delta t$  from the distribution at  $t$  as

$$f_i(\vec{x} + c\vec{e}_i\Delta t, t + \Delta t) = f_i(\vec{x}, t) - \frac{f_i(\vec{x}, t) - f_i^{eq}(\vec{x}, t)}{\tau}. \quad (7)$$

$f_i^{eq}$  is evaluated from the macroscopic density and velocity as

$$f_i^{eq}(\vec{x}, t) = \omega_i \rho \left( 1 + 3 \frac{\vec{e}_i \cdot \vec{v}}{c^2} + \frac{9}{2} \frac{(\vec{e}_i \cdot \vec{v})^2}{c^4} - \frac{3}{2} \frac{\vec{v} \cdot \vec{v}}{c^2} \right), \quad (8)$$

where  $\omega_i$  are weight factors:  $\omega_i = 4/9$  for  $i = 0$ ,  $\omega_i = 1/9$  for  $i = 1, 2, 3, 4$  and  $\omega_i = 1/36$  for  $i = 5, 6, 7, 8$ . In the previous equation  $c = \Delta x/\Delta t$  is the lattice speed, which is taken to be 1. Another relation links the fluid kinematic viscosity  $\mu$  to the relaxation time  $\tau$  by

$$\mu = \frac{2\tau - 1}{6} \frac{(\Delta x)^2}{\Delta t}. \quad (9)$$

The first term of the second member of Eq. 7 refers to the streaming phase, while the second one to the collision phase. These two phases are generally separated in the programming process. Two types of boundary conditions are introduced in our model. The first one concerns the reflection of the particles on the fixed obstacles (the fibers of the porous samples). A full-way model of bounce-back is preferred to a mid-way bounce-back model since the first does not require to know the normal orientation when a particle enters in contact with a rigid boundary. This model is adapted when several obstacles are present. The fixed lattice nodes in contact with the wet area are to be considered in the streaming process, at a first step, next to the particle distribution functions of these nodes pointing to the exterior of the fluid area, reversed in direction. The second type of boundary condition are inputs, which are generally imposed pressure or imposed velocity. In our case, we intend, from the definition of the permeability (Eq. 1), to impose a pressure gradient (a body force) all over the fluid domain. This leads to non-trivial developments studied in.<sup>5</sup> The body forces have to be added to the initial equilibrium Eq. 6:

$$f_i(\vec{x} + c\vec{e}_i\Delta t, t + \Delta t) - f_i(\vec{x}, t) = -\frac{f_i(\vec{x}, t) - f_i^{eq}(\vec{x}, t)}{\tau} + \Delta t F_i, \quad (10)$$

where  $F_i$  are the body forces. Theoretically, all previous formulae (5) to (8) should be modified. However,<sup>5</sup> shows that when the body forces are slightly changing in space and time, the representation of the body as  $F_i = \omega_i \vec{e}_i \cdot \vec{F} / c_s^2$  can be directly introduced in the previous model unaltered, and the Navier-Stokes equations remain verified. Finally, using the notation  $:=$  as the programming affectation operator, our algorithm for a current iteration is as follows:

- LBM algorithm

$$\begin{aligned} f_i(\text{iter} + 1) &:= Pr(f_i(\text{iter})) \text{ (propagation);} \\ f_i(\text{iter} + 1) &:= f_i(\text{iter} + 1) + F_i, \text{ (body forces);} \\ f_i(\text{iter} + 1) &:= Bb(f_i(\text{iter} + 1)) \text{ (bounce-back);} \\ \rho &:= \sum_i f_i(\text{iter} + 1); \quad \vec{v} := \sum_i f_i(\text{iter} + 1)\vec{e}_i / \rho \text{ (macro);} \\ f_i^{eq}(\rho, \vec{v}) &\text{ (equilibrium);} \\ f_i(\text{iter} + 1) &:= f_i(\text{iter} + 1) - \frac{f_i(\text{iter}+1) - f_i^{eq}}{\tau} \text{ (collision).} \end{aligned}$$

Many studies using LBM concern the enhancement of the method, and their results are presented in Lattice units. To solve physical problems, physical units shall be converted to Lattice units and, next, shall express the LBM results in physical units. The conference paper<sup>7</sup> focuses on this aspect and presents a clear methodology. Conversion factors are established for the fundamental entities, L (length), M (mass), and T (time). Conversion for secondary entities such as pressure or velocity are deduced from the previous factors. Three independent primary conversion factors are needed, chosen to be, in our case, length, dynamic viscosity and density. The pre-process to LBM algorithm (Physical to LBM units) is given hereafter, where the 2D image has a resolution of (NX\*NY) pixels and the pixel size is known. Phys refers to physical units, and Lat to Lattice units.

- From physical to LBM units

-> Physical

$$PhysH := NY * PixelSize \text{ (m) (imposed by the image)}$$

$$PhysDynVisco := 1.84e^{-5} \text{ (Pa/s)}$$

$$PhysDensity := 1.225 \text{ (kg/m}^3\text{)}$$

$$PhysGravity := 9.81 \text{ (m/s}^2\text{)}$$

$$PhysKinVisco := PhysDynVisco / PhysDensity \text{ (m}^2\text{/s)}$$

-> Lattice

$$LatH := NY$$

$$LatDensity := 1.0$$

$$LatTau := 0.66 \text{ (chosen by the user)}$$

-> Conversion such as  $PhysQ = LatQ * CoefQ$

$$CoefH := PhysH / LatH$$

$$CoefDensity := PhysDensity / LatDensity$$

SHORT PAPER TITLE

$$LatKinVisco := (LatTau - 0.5)/3.0$$

$$CoefT := LatKinVisco * CoefH * CoefH / PhysKinVisco$$

-&gt; Coefficients deduced

$$CoefU := CoefH / CoefT$$

$$CoefF := CoefDensity * (CoefH)^4 / (CoefT)^2$$

-&gt; Other

$$PhysdPdL := 20.0 (Pa/m) \text{ (chosen by the user)}$$

$$LatdPdL := PhysdPdL / CoefDensity / CoefH * CoefT * CoefT$$

From this, the LBM algorithm is applied, and the Darcy's permeability,  $Lat2DK0DarcyPorous$ , evaluated in Lattice units. The post-process to the LBM algorithm (LBM to Physical units) in order to deduced the resistivity in physical unit is as follows:

- From LBM to physical units

$$Phys2DK0 = CoefH * CoefH * Lat2DK0DarcyPorous (m^2)$$

$$Phys2DRes = PhysDynVisco / Phys2DK0 (Pa.s/m^2)$$

$$Phys3DRes = Phys2DRes / correctiveFactor (Pa.s/m^2)$$

The full script of our MATLAB© code is in the open domain and can be found in the following repository (<http://www.labvib.ufc.br/CavLBM.html>).

The visualization of the velocity field is followed up from time to time during the iteration process. Convergence is generally obtained within 5000 iterations and lasts 5 minutes using a common Laptop computer. What is observed is that iteration by iteration the streamlines re-enforce up to convergence. Fig. 8 shows theses streamlines.

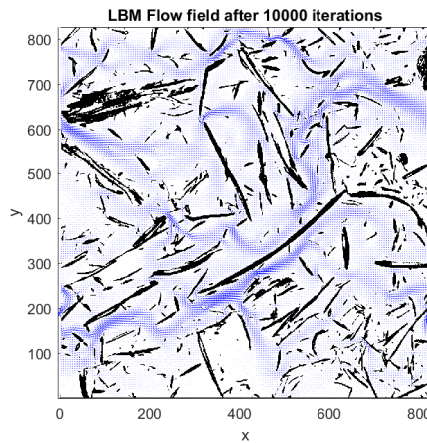


Figure 8: Flow field streamlines through a porous sample.

#### 4. Results and discussion

A set of 10 slices is analysed. The first slice, numbered 150, is selected; next, the slices 200, 300, ..., 900 and 939 (the last one) are selected. For each slice, the porosity and the resistivity are calculated. For the resistivity, both directions, 1 and 2, are considered. The results are reported in Table 1, where the lowest and highest value of the porosity are, respectively, 0.84 and 0.87 with a mean value of  $0.860 \pm 0.09$ . For the resistivity, the lowest and highest value are, respectively,  $807.84 Pa.s/m^2$  and  $2238.55 Pa.s/m^2$  with a mean value of  $1346 \pm 12 (Pa.s/m^2)$ . The results are found very consistent compared to the results obtained using a porosity-meter, 0.866, and a resistivity-meter,  $1350 Pa.s/m^2$ . These reference values are labelled as RefTest in Table 1.

**Table 1: LBM analysis of 10 slices.**

Sample	Porosity	Res. (Dir1)	Res. (Dir2)
150	0.8423	2238.55	2082.37
200	0.857	1216.15	1308.99
300	0.844	1678.57	1479.85
400	0.873	1141.33	875.66
500	0.868	1001.29	1253.72
600	0.862	1028.52	1253.73
700	0.861	1994.88	1368.00
800	0.865	1065.42	998.63
900	0.864	807.84	1306.30
939	0.867	1121.50	1318.68
Mean	$0.860 \pm 0.09$	$1346 \pm 12$	
RefTest	0.866	1350	

## 5. Conclusions

According to our knowledge, this the first time that the LBM method is experimented to compute the static airflow resistivity of highly porous materials used in acoustics. A simple 2D implementation of the LBM was built for this purpose and is applied to tomographic 2D images of a porous fibrous sample. Images are first processed to obtain black and white images from which the porosity of the sample is evaluated. Next, the pixels images are directly used as the lattice of the LBM to compute the static airflow resistivity. We found the results very consistent with measurements using a porosity-meter and an airflow resistivity-meter. The numerical approach led to a porosity of 0.86 and a resistivity of  $1346 Pa.s/m^2$ , while the directly measured values were 0.87 and  $1350 Pa.s/m^2$ , respectively. It suggests the potential capability of the approach combining Tomography and LBM calculations to characterize other fibrous materials. A 3D implementation of the LBM should follow.

## 6. Acknowledgments

The authors would like to thank the CAPES-COFECUB Project 773/13 - Proc. 8909-14-8 , the CNPq/Universal Proc. 82351/2013-6 and the CAPES/PNPD Proc. 1564115 for their financial support. We would also like to thank Jean-Daniel Chazot, from the Laboratoire Roberval (UMR CNRS 7337) of the Université de Technologie de Compiègne (UTC)/France, and Benjamin Smaniotto, Technical Manager of the tomograph of the Laboratoire de Mécanique et Technologie (LMT, UMR CNRS 8535) of the ENS Paris-Saclay, for their valuable help.

## References

- [1] AFPC-AFREM. Détermination de la masse volumique apparente et de la porosité accessible à l'eau - méthodes recommandées pour la mesure des grandeurs associées à la durabilité. In *Compte-rendu des Journées Techniques, Toulouse, 11-12 Décembre 1997*, pages 121–124, 1997.
- [2] J. F. Allard and N. Atalla. *Propagation of Sound in Porous Media: Modeling Sound Absorbing Materials*. 2nd Edition, Wiley, 2009.
- [3] Y. Bao and J. Meskas. Lattice boltzmann method for fluid simulations. Technical report, New York University, Department of Mathematics, 2011.
- [4] C. Van der Kelena and P. Göransson. Identification of the full anisotropic flow resistivity tensor for multiple glass wool and melamine foam samples. *JASA*, 134:46–59, 09 2013.
- [5] Z. Guo, C. Zheng, and B. Shi. Discrete lattice effects on the forcing term in the lattice boltzmann method. *PHYSICAL REVIEW E*, 65, 046308, 04 2002.
- [6] A. Keller. High resolution, non-destructive measurement and characterization of fracture apertures. *Int. Journal Rock Mech. Min. Sci.*, 35(8):1037–1050, 1998.

SHORT PAPER TITLE

- [7] T. Krüger. Unit conversion in lbm. In *LBM Workshop, Edmonton, Canada*, 08 2011.
- [8] Y. Salissou and R. Panneton. Pressure/mass method to measure open porosity of porous solids. *J. Appl. Phys.*, 101, 2007, 124913: 1-7., 2007.
- [9] H. Taud, R. Martinez-Angeles, J. F. Parrot, and L. Hernandez-Escobedo. Porosity estimation method by x-ray computed tomography. *J. Petroleum Sci. and Eng.*, 47:209–217, 2005.
- [10] P. Wang. Lattice boltzmann simulation of permeability and tortuosity for flow through dense porous media. *Mathematical Problems in Engineering*, Article ID 694350, 07 2014.